Expression and Mutagenesis of the Sea Anemone Toxin Av2 Reveals Key Amino Acid Residues Important for Activity on Voltage-Gated Sodium Channels †

ARTICLE *in* BIOCHEMISTRY · AUGUST 2006

Impact Factor: 3.02 · DOI: 10.1021/bi060386b · Source: PubMed

6 AUTHORS, INCLUDING:

Yehu Moran
Hebrew University of Jerusalem
25 PUBLICATIONS **405** CITATIONS
SEE PROFILE

Lior Cohen
Hebrew University of Jerusalem
32 PUBLICATIONS **882** CITATIONS
SEE PROFILE

Roy Kahn
InSight Biopharmaceuticals Ltd.
22 PUBLICATIONS **500** CITATIONS
SEE PROFILE

Dalia Gordon
Weizmann Institute of Science
126 PUBLICATIONS **4,144** CITATIONS
SEE PROFILE

Expression and Mutagenesis of the Sea Anemone Toxin Av2 Reveals Key Amino Acid Residues Important for Activity on Voltage-Gated Sodium Channels†

Yehu Moran, Lior Cohen, Roy Kahn, Izhar Karbat, Dalia Gordon,* and Michael Gurevitz*

Department of Plant Sciences, George S. Wise Faculty of Life Sciences, Tel-Aviv University, Ramat-Aviv 69978, Tel-Aviv, Israel

Received February 26, 2006; Revised Manuscript Received May 28, 2006

ABSTRACT: Type I sea anemone toxins are highly potent modulators of voltage-gated Na-channels (Na_vs) and compete with the structurally dissimilar scorpion alpha-toxins on binding to receptor site-3. Although these features provide two structurally different probes for studying receptor site-3 and channel fast inactivation, the bioactive surface of sea anemone toxins has not been fully resolved. We established an efficient expression system for Av2 (known as ATX II), a highly insecticidal sea anemone toxin from *Anemonia viridis* (previously named *A. sulcata*), and mutagenized it throughout. Each toxin mutant was analyzed in toxicity and binding assays as well as by circular dichroism spectroscopy to discern the effects derived from structural perturbation from those related to bioactivity. Six residues were found to constitute the anti-insect bioactive surface of Av2 (Val-2, Leu-5, Asn-16, Leu-18, and Ile-41). Further analysis of nine Av2 mutants on the human heart channel $Na_v1.5$ expressed in *Xenopus* oocytes indicated that the bioactive surfaces toward insects and mammals practically coincide but differ from the bioactive surface of a structurally similar sea anemone toxin, Anthopleurin B, from *Anthopleura xanthogrammica*. Hence, our results not only demonstrate clear differences in the bioactive surfaces of Av2 and scorpion alpha-toxins but also indicate that despite the general conservation in structure and importance of the Arg-14 loop and its flanking residues Gly-10 and Gly-20 for function, the surface of interaction between different sea anemone toxins and Na_vs varies.

Sea anemones (Anthozoa) of the Cnidarians have appeared 540 million years ago (*1*). They are sessile carnivores that heavily depend on their venom for prey and defense. The venom consists of numerous toxin types, some of which act on voltage-gated sodium channels (Na_vs[1]). Na_vs have a pivotal role in animal neuronal excitability and, therefore, are targeted by a large variety of toxins used by many organisms (*2*). Na_vs are composed of a pore-forming α-subunit (260 kDa) associated with one or two *β*-subunits. The α-subunit consists of four domains (D1−D4), each made of six trans-membrane segments (S1−S6) connected by internal and external loops. A prominent characteristic of Na_vs is their ability to rapidly activate and inactivate upon cell membrane depolarization, leading to a transient increase in Na^+ conductance (*3*, *4*).

Among sea anemone toxins that affect Na_vs, the most studied group is Type I. These are 47−51 amino acids long peptides reticulated by three disulfide bridges (Figure 1), which contain a flexible loop encompassing residues 8−17, named after the conserved Arg in its center (*5*). These toxins bind to a Na_v region named receptor site-3, which is also recognized by scorpion α-toxins (*6*−*8*). Mutations in the short S3−S4 loop in domain 4 (D4/S3−S4) of $Na_v1.2a$ (a brain channel subtype) were shown to affect the binding of the sea anemone toxin ATX II (renamed here as Av2: *Anemonia viridis* toxin 2) and the scorpion α-toxin Lqq5 (from *Leiurus quinquestriatus quinquestriatus*), leading to the proposal that D4/S3−S4 may be part of receptor site-3 (*9*). The physiological effects on the channel by both sea anemone and scorpion α-toxins are very similar and are characterized in whole-cell patch clamp measurements by currents lasting far beyond the point in time when untreated channels have gone through inactivation (*2*).

Av2 is the most abundant and lethal neurotoxin found to date in the venom of the sea anemone *Anemonia viridis* (*10*). This toxin was shown to have a strong effect on crustaceans and insects and a weaker effect on mammals (*10*, *11*). When tested on $DmNa_v1$ (*Drosophila melanogaster* Na_vs) expressed in *Xenopus laevis* oocytes, Av2 strongly inhibited channel inactivation, as expected for a site-3 toxin (*12*), whereas the effect on $Na_v1.2a$ was much weaker. Using various test systems, it has also been shown that this toxin and other Type I toxins strongly affect the cardiac muscle Na_v (*13*, *14*).

† This research was supported by the United States−Israel Binational Agricultural Research and Development Grant IS-3480-03 (to M.G. and D.G.), the Israeli Science Foundation Grants 909/04 (to M.G.) and 1008/05 (to D.G.), and by Grant No. G-770-242.1/2002 (to D.G.) from the German-Israeli Foundation (G. I. F.) for Scientific Research and Development.

* To whom correspondence should be addressed. Tel: 972-3-6409844. Fax: 972-3-6406100. E-mail address: mamgur@post.tau.ac.il (M.G); dgordon@post.tau.ac.il (D.G).

[1] Abbreviations: ApA, Anthopleurin A; ApB, Anthopleurin B; Av2, *Anemonia viridis* toxin 2; CD, circular dichroism; D4/S3−S4, a loop between segments 3 and 4 in the 4th domain of voltage-gated sodium channels; MALDI-TOF, matrix assisted laser desorption ionization-time-of-flight; Na_v, voltage-gated sodium channel; nAv2 and rAv2, native and recombinant Av2.

10.1021/bi060386b CCC: $33.50
Published on Web 07/01/2006

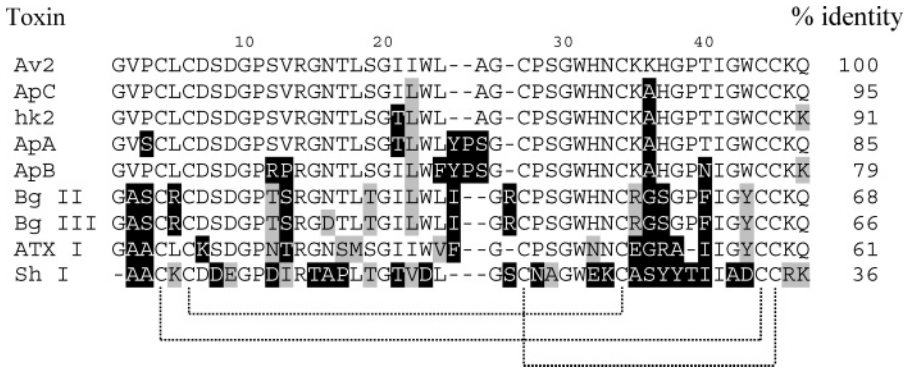

FIGURE 1: Sequence alignment of sea anemone toxin representatives. The sequences are aligned according to the conserved cysteine residues, which form disulfide bonds (dotted lines below the sequences). The dashes indicate gaps, and the numbering follows Av2. The gray and black boxes represent conservative and nonconservative substitutions. Av1 (= ATX Ia) and Av2 are from *Anemonia viridis* (formerly named *Anemonia sulcata*); Bg II is from *Bunodosoma granulifera*; ApA and ApB are from *Anthopleura xanthogrammica*; ApC is from *Anthopleura elegantissima*; hk2 is from an *Anthopleura* uncharacterized species; Sh I, is a Type II sea anemone toxin from *Stichodactyla helianthus*; Bg II and Bg III sequences are taken from ref 19; hk2 sequence is taken from ref 17; and all other toxin sequences appear in ref 5.

Sea anemone toxins attracted attention because of their strong effect and preference for distinct channel types. Chemical modifications in Av2 pointed out the putative importance of Gly-1, Lys-35, Lys-36, Lys-46, His-32, and His-37 for binding affinity and toxicity toward crabs and rats (*15*). Moreover, an amine bond formed between the carboxyl groups of Asp-7, Asp-9, and Gln-47 (*C*-terminus) and a glycine ethyl ester banished the toxicity and did not affect the binding affinity for rat brain synaptosomes (*15*).

Anthopleurin B (ApB), a toxin from the sea anemone *Anthopleura xanthogrammica*, which shares 79% identity with Av2 (Figure 1), was expressed in *Escherichia coli* (*16*) and mutagenized. The effects of the recombinant toxin and its mutants on $Na_v1.2$ and $Na_v1.5$ (a cardiac muscle channel subtype) were analyzed in order to identify mutations that increase its preference for the cardiac muscle Na_v. These studies have suggested a bioactive role for Arg-12, Asn-16, Leu-18, Ser-19, Lys-37, Trp-33, and Lys-49 (*2*). Recently, four toxins from Chinese *Anthopleura* species (hk toxins; see Figure 1 for hk2) have been expressed in *E. coli* and tested on isolated rat atria. A comparative analysis of their effects on the contraction of the atria suggested that residues at positions 14, 22, 25, and 37, which vary in these toxins, are involved in their action (*17*). Thus, despite the high sequence identity (Figure 1) and structural similarity, the chemical modification of Av2, the mutagenesis of ApB, and the comparison of the natural hk variants could imply that their bioactive surfaces toward mammalian Na_vs vary greatly (*2*, *15*, *17*). Yet, a more conclusive description of these surfaces requires a comparison based on similar methods of modification.

Channel residues that may interact with Av2 have been first proposed by Rogers et al. (*9*). By the mutagenesis of residues in the extracellular loops of the rat brain channel $Na_v1.2a$, Glu-1613, Val-1620, and Leu-1624 were suggested to be involved in toxin recognition. Later on, Lys-37 of ApB (equivalent to Lys-35 in Av2) was proposed to interact directly with Asp-1612 (equivalent to Glu-1613 of $Na_v1.2a$) of the heart channel $Na_v1.5$ (*18*).

The comparison of structures of the anti-mammalian scorpion α-toxin Aah2 (from *Androctonus australis hector*) and the sea anemone toxin Bg II (from *Bunodosoma granulifera*) has led to the assumption that the Arg-5, Arg-14, Arg-27, and Arg-36 quartet, together with the hydrophobic Trp-32 on the surface of Bg II, are spatially similar to Arg-62, Lys-58, Lys-50, Arg-18, and Tyr-47, respectively, on the surface of Aah2 and, hence, may account for their ability to compete for the same receptor site (*19*). Besides that for Arg-36 (parallel to Lys-37 in ApB), this assumption was not supported by data obtained later from the mutagenesis of ApB (*18*).

The results of previous studies of sea anemone toxins revealed residues important for activity on mammalian Na_vs, but did not provide a complete picture of the entire bioactive surface or the residues important for activity on insect Na_vs. Intrigued by the strong potency and noticeable preference of sea anemone toxins for insect Na_vs, we established an efficient expression system in *E. coli* for Av2 and mutagenized its entire surface. This molecular dissection revealed a bioactive surface toward insect Na_vs quite similar to the bioactive surface toward mammalian heart Na_vs. These surfaces differ significantly from that proposed for ApB toward mammalian Na_vs and from that elucidated in scorpion α-toxins toward insects.

EXPERIMENTAL PROCEDURES

Bacterial Strains, Animals, and Native Av2. The *Escherichia coli* strain DH5α was used for plasmid constructions, and the BL21 strain (DE3, pLys) was used for toxin expression by the His-tag carrying vector pET-14b (Novagen, Madison, WI) in a protocol similar to that described previously (*20*, *21*). *Sarcophaga falculata* blowfly larvae were bred in the laboratory. Native Av2 (nAv2) was purchased from Latoxan (Valence, France).

Construction of the Av2 Gene. A synthetic gene encoding for Av2 was planned according to the published amino acid sequence (*22*). The gene was constructed using six overlapping oligonucleotide primers designed with a codon usage based on the nucleotide sequence of toxin genes that have been successfully expressed in *E. coli* (*20*, *21*): (primer 1) 5′-CATATGGGTGTACCTTGCCTATGCGACAGCGACGGTCCTAGCGTTCGAGGTAACACACTA-3′, (primer 2) 5′-TCGGGTATTATCTGGCTAGCTGGTTGCCCTAGCGGTTG-3′, (primer 3) 5′-GCATAACTGCAAGAAGCATGGTCCTACGATTGGTTGGTGCTGCAAGCAGTAAGGATCC-3′,

(primer 4) 5′-GGATCCTTACTGCTTGCAGCACCAAC-CCGTAGGACCATGCTT-3′, (primer 5) 5′-CTTGCAGTT-ATGCCAACCGCTAGGGCAACCAGCTAGCCAGATAATACCCG-ATAGTGTGT TACC-3′, (primer 6) 5′-TCGAACGCTAG-GACCGTCGCTGTCGCATAGGCAAGGTACACCCATATG-3′. A mixture of 1 μM each of the six primers was heated to 95 °C and then cooled stepwise to 4 °C for annealing. The mixture was diluted 1:40 in the ligation buffer, and 40 units of T4 ligase (Roche, Indianapolis, IN) was added for overnight reaction at 15 °C. The ligation mixture (1 μM) was used for PCR amplification of the Av2 gene using (primer 7) 5′-TTCATATGGGTGTACCTTGCCT-3′, which included an NdeI restriction site at the start of the gene, and (primer 8) 5′-TTGGATCCTTACTGCTTGCAGC-3′, which contained a BamHI restriction site downstream to the gene. The PCR product was phosphorylated by polynucleotide kinase (New England Biolabs, Ipswich, MA) and cloned into the SmaI site of pBluescript (Stratagene, La Jolla, CA). After sequence verification, the NdeI−BamHI fragment was cleaved and subcloned into the corresponding sites of pET-14b.

Expression and Production of Recombinant Av2. pET-14b carrying the Av2 gene was used to transform *E.* coli BL21 cells. The recombinant protein accumulated as inclusion bodies was isolated by differential centrifugation, denatured by 6 M guanidinium hydrochloride, and folded in vitro as was previously described for a scorpion toxin (*23*). After folding, the toxin was purified by reverse-phase high performance liquid chromatography using a Resource column (Amersham Biosciences, Björkgatan, Sweden) with a gradually rising gradient of acetonitrile (28−33%). A major peak of Av2 was eluted from the column by 30% acetonitrile. The average yield of His-Av2 was 1.5 mg from 1 L of *E. coli* culture. The His-tag was cleaved using 1 unit of thrombin (Sigma, St. Louis, MO) per 150 μg of His-tag protein. The cleaved product was purified by the same method as that used for the His-tag protein.

Mutagenesis. Mutations in Av2 were introduced via PCR using complementary oligonucleotide primers and the constructed Av2 gene as the DNA template. All toxin mutants were produced in a fashion similar to that used for the unmodified toxin.

Toxicity Assays. Four-day-old blowfly larvae (*S. falculata* 150±20 mg of body weight) were injected intersegmentally. A positive result was scored when immobilization and contraction were observed after 10 min, which was slower than the effect induced by the anti-insect scorpion α-toxin LqhαIT. Five concentrations of each toxin were injected into larvae (nine larvae in each group) in three independent experiments. Effective dose 50% (ED_{50}) values were calculated according to the sampling and estimation method of Reed and Muench (*24*).

Competition Binding Experiments. Neuronal membranes were prepared from the heads of adult *Periplaneta americana* cockroaches (*25*). Membrane protein concentration was determined by a Bio-Rad Protein Assay, using bovine serum albumin (BSA) as the standard. Radioiodinated LqhαIT was prepared by lactoperoxidase (Sigma, St. Louis, MO; cat. no., L8257; 7 units/60 μL of reaction mix) using 10 μg of toxin and 0.5 mCi carrier-free $Na^{125}I$ (Amersham, Chalfont St. Giles, U.K.) following a published protocol (*26*). The monoiodotoxin was purified using an analytical Resource RP-HPLC column (6.4 × 100 mm, 15 μm particle size; Amersham, Björkgatan, Sweden). The concentration of the radiolabeled toxin was determined according to the specific radioactivity of the ^{125}I corresponding to 2500−3000 dpm/fmol of monoiodotoxin, depending on the age of the radiotoxin and the estimation of its biological activity (usually 70−80%; (*25*)). The composition of media used in the binding assays and the termination of the reactions has been previously described (*25*). Nonspecific toxin binding was determined in the presence of excess (1 μM) unlabeled toxin. The equilibrium competition binding assays were performed using increasing concentrations of unlabeled toxin in the presence of a constant low concentration of ^{125}I-LqhαIT (0.05−0.1 nM) and analyzed by the computer program KaleidaGraph (Synergy Software, U.S.A.) using a nonlinear Hill equation (for IC_{50} determination). The K_i values were calculated by the equation $K_i = IC_{50}/(1 + (L^*/K_d))$, where L^* is the concentration of the radioiodinated toxin, and K_d is its dissociation constant. Each experiment was performed in duplicate and repeated at least three times as indicated (n). Data are presented as the mean ± SE of the number of independent experiments (*25*). The binding energy of toxin variants was calculated from the equation $\Delta\Delta G = -RT \ln(K_i^{wt}/K_i^{mut})$.

CD Spectroscopy. CD spectra were recorded at 25 °C using a model 202 circular dichroism spectrometer (Aviv Instruments, Lakewood, NJ). The toxins (150 μM) were dissolved in 5 mM sodium phosphate buffer at pH 7.0, and their spectra were measured using a quartz cell of 0.1-mm light path. Each spectrum was measured three times and averaged, and a blank spectrum of the buffer that was run under identical conditions was subtracted.

Electrophysiological Assays. cRNAs encoding the human heart ($Na_v1.5$) and *Drosophila melanogaster* para ($DmNa_v1$) sodium channel α-subunits and the auxiliary subunits β1 and TipE were transcribed in vitro using T7 RNA-polymerase and the mMESSAGE mMACHINE system (Ambion, Austin, TX; (*27*, *28*)) and injected into *Xenopus laevis* oocytes as was described (*29*). Currents were measured 1−4 days after injection using a two-electrode voltage clamp and a Gene Clamp 500 amplifier (Axon Instruments, Union City, CA). Data were sampled at 10 kHz and filtered at 5 kHz. Data acquisition was controlled by a Macintosh PPC 7100/80 computer, equipped with ITC-16 analog/digital converter (Instrutech Corp., Port Washington, NY), utilizing Synapse (Synergistic Systems, Sweden). Capacitance, transient, and leak currents were removed by subtracting a scaled control trace utilizing a P/6 protocol (*28*). The oocytes were washed with bath solution (in mM: 96 NaCl, 2 KCl, 1 $MgCl_2$, 2 $CaCl_2$, 5 HEPES at pH 7.85) flowing from a BPS-8 perfusion system (ALA Scientific Instruments, Westbury, NY) with 4 psi positive pressure. The toxins were diluted with bath solution containing 1 mg/mL of BSA and applied directly to the bath to the final desired concentration. To discard any application-derived artifacts, 1 mg/mL of BSA solution was applied before the toxin was added. To obtain a dose−response curve, the currents were elicited by depolarization to −10 mV from a holding potential of −80 mV in the presence of several toxin concentrations. At each toxin concentration, the currents were allowed to reach a steady-state level prior to the final measurement. The dose-dependent effect of the toxin (removal of fast inactivation)

Table 1: Insecticidal and Anti-Mammalian Effects of Sea Anemone and Scorpion α-Toxins[a]

toxin	ED_{50} for *S. falculata* (pmol/g body weight)	LD_{50} for *B. germanica* (pmol/g body weight)	LD_{50} for mice[b] (pmol/g body weight)
nAv2	3.7	2.5[c]	22[d]
His-Av2	21		
rAv2	3.4		
LqhαIT	17	2.5[c]	8.3[c]
Aah2		897[c]	1.7[c]

[a] Effect of toxins in insects was determined by injections to blowfly larvae (*Sarcophaga falculata*) and/or cockroaches (*Blatella germanica*). nAv2, native toxin; His-Av2, toxin fused to a His-tag; rAv2, His-Av2 cleaved by thrombin; LqhαIT, the highly insecticidal α-toxin from the scorpion *Leiurus quinquestriatus hebraeus;* Aah2, an anti-mammalian α-toxin from the scorpion *Androctonus australis hector*. [b] Subcutaneous injection. [c] Ref 8. [d] Ref 15.

was calculated by plotting the ratio of the steady-state current measured 50 ms after depolarization (I_{ss}) to the peak current (I_{peak}) as a function of toxin concentration and fitting with the Hill equation: $I_{ss}/I_{peak} = a_0 + (a_1 - a_0)/[1 + (EC_{50}/[\text{toxin}])]^H$, where H is the Hill coefficient, [toxin] is the toxin concentration, and a_0 is the offset measured prior to toxin application. The amplitude $a_1 - a_0$ provides the maximal effect obtained at saturating toxin concentration. EC_{50} is the toxin concentration that causes half-maximal inhibition of fast inactivation. To minimize variability, H was set to 1 in all calculations.

Mass Spectrometry, The mass of representative Av2 mutants (after thrombin cleavage) was determined at the Maiman Proteome Research Institute, Tel-Aviv University, using a Voyager DE-STR MALDI-TOF mass spectrometry system (Applied Biosystems, Foster City, CA).

Three-Dimensional Models. The 3-D models were drawn using DeepView/PDB viewer (version 3.7 by GSK) and were rendered by PovRay (version 3.6 by Persistence of Vision Raytracer, Ltd.). The 3-D model of Av2 was constructed using the SWISS-MODEL structure homology-modeling server (www.expasy.org/swissmod/SWISS-MODEL.html; (*30*)) according to the following structures of sea anemone toxins: 1ah1_.pdb, 1apf_.pdb, 1atx_.pdb, 1shl_.pdb, 1shi_.pdb, 2shl_.pdb. The models are ordered according to their contribution to the Av2 model. All six models are available at the Protein Data Bank (https://www.pdb.org).

RESULTS

Characterization of the Recombinant Av2. The recombinant Av2 with a His-tag at its *N*-terminus was examined by SDS−PAGE, amino acid composition analysis, and MALDI-TOF mass spectrometry (data not shown). The His-tag was cleaved by thrombin, and the physical properties of the resulting protein (rAv2), bearing an *N*-terminal addition of Gly, Ser, His, and Met, were verified again.

Both His-Av2 and rAv2 were active and induced contraction symptoms in *S. falculata* larvae similar to those obtained with native Av2 (nAv2) isolated from the sea anemone venom. Whereas rAv2 was equally toxic to nAv2, His-Av2 was 5.5-fold weaker (Table 1). Notably, Av2 was more effective in these larvae than any of the known scorpion toxins, and although its effect developed relatively slow, it was irreversible. The physiological effects of nAv2 and rAv2

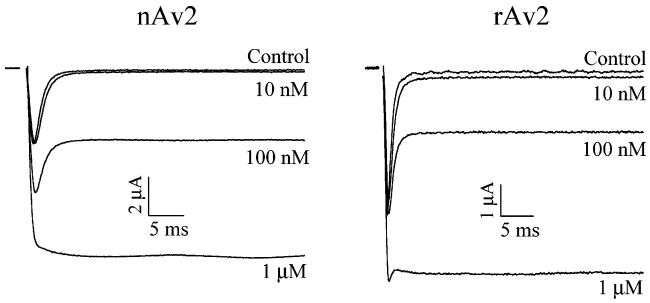

FIGURE 2: Effects of nAv2 and rAv2 on currents mediated by the $DmNa_v1$ channel expressed in *Xenopus laevis* oocytes. The oocytes were clamped at −80 mV, and currents were elicited by step depolarizations to −10 mV. Upon toxin application to the bath solution, a component of noninactivating current has gradually developed reaching saturation at a concentration of 1 μM toxin.

on the insect Na_v were compared using the *Drosophila* para sodium channel, $DmNa_v1$ expressed together with its auxiliary TipE subunit in *Xenopus* oocytes. The oocytes were held at −80 mV, and a 50 ms test pulse to −10 mV was applied to elicit sodium currents. As shown in Figure 2, the inhibition of inactivation obtained in the presence of identical concentrations of these toxins was very similar. In competition binding assays using ^{125}I-LqhαIT as a marker for receptor site-3 (*7*), His-Av2, rAv2, and nAv2 were very similar and provided K_i values of (in nM) 0.41 ± 0.02 ($n = 3$), 0.22 ± 0.14 ($n = 3$), and 0.4 ± 0.05 ($n = 3$), respectively (Figure 3A). These results have shown that the additional residues at the *N*-terminus had only a slight effect on the binding affinity of Av2. These analyses indicated that the recombinant Av2 was as potent as the native toxin, which paved the way for further analysis by mutagenesis.

Analysis of the Av2 Surface by Mutagenesis. All residues excluding Cys and a number of Gly were Ala scanned. The mutant toxins were produced and purified in a manner similar to that used for His-Av2, and each was analyzed by toxicity assays on *S. falculata* larvae and binding assays using neuronal membranes of *P. Americana* (Figure 3A). The effects on toxicity correlated well with the results of the binding assays, and therefore, the results presented hereafter are those of the apparent binding affinity. All mutants whose binding affinity decreased significantly ($\Delta\Delta G$ >1.3 kcal/mol; Table 2 and Figure 3B) were cleaved by thrombin, purified, and compared to that of rAv2. To reassure that the results obtained for the His-mutants were reliable, the His-tag was also cleaved in a few mutant representatives whose activity was unaffected, and they were compared with that of rAv2. In all cases, the ED_{50} ratio and $\Delta\Delta G$ have not changed significantly, indicating that the small decrease in activity due to the His-tag was equal in the mutants. To discern between mutations that changed the activity because of structural perturbation from those directly involved in the interaction with the channel receptor, the CD spectrum of each toxin mutant was analyzed. The vast majority of the substitutions to Ala (24 out of 30) had no significant effect on the toxicity and binding affinity of Av2, and the CD spectrum of the mutants was similar to that of the unmodified toxin (Figure 4).

Analysis of Residues that Constitute the N-Terminal Segment of Av2. Mutagenesis indicates that two of the nine residues that constitute the *N*-terminal region in Av2, Val-2, and Leu-5 play a role in activity (Table 2). These results

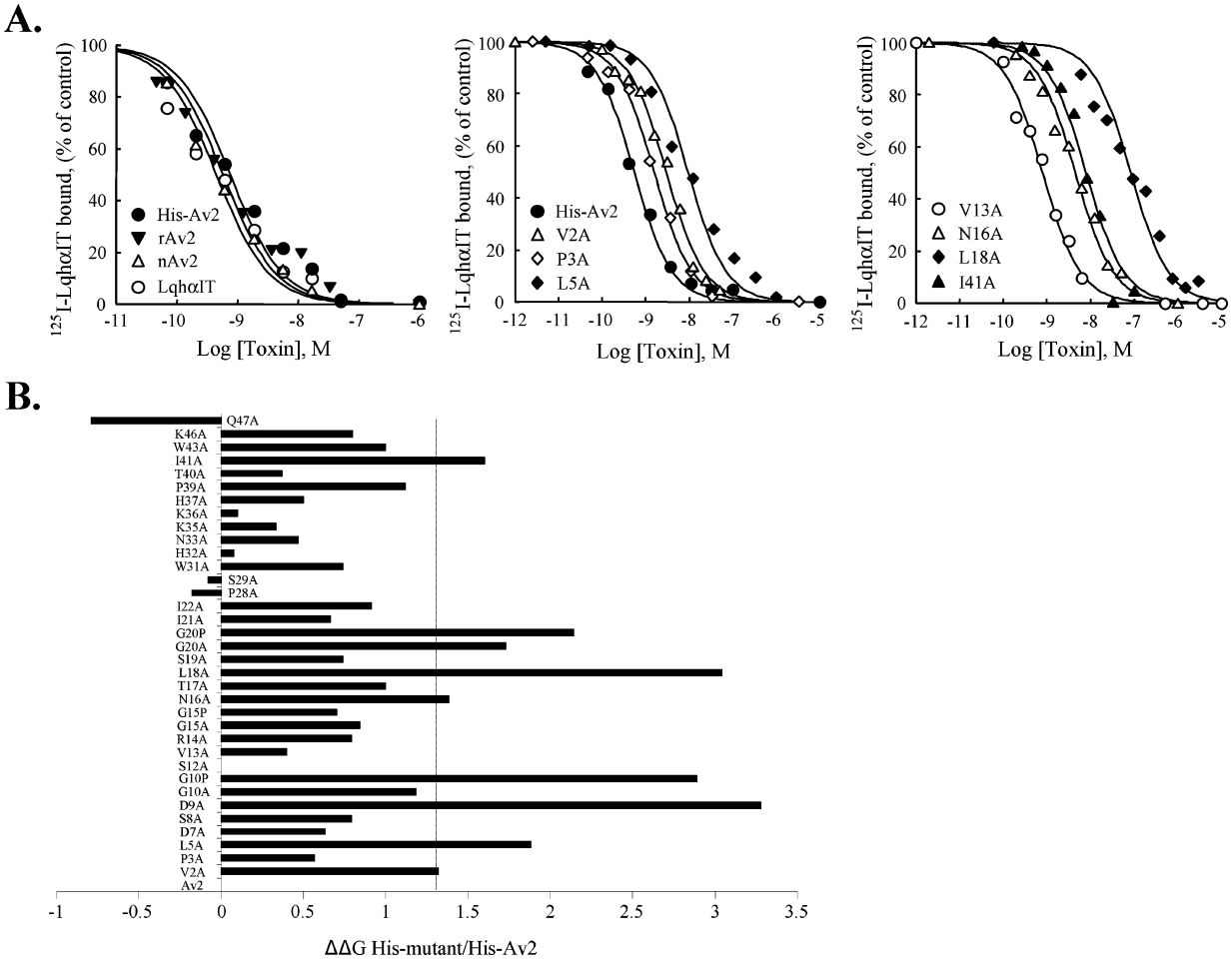

FIGURE 3: Mutagenic dissection of Av2. (A) Competition of His-Av2 mutants with ^{125}I-LqhαIT on binding to cockroach neuronal membranes. Representative experiments are shown. The membranes (7 μg/mL) were incubated for 60 min at 22 °C with 0.1 nM ^{125}I-LqhαIT, and increasing concentrations of the various mutants. Nonspecific binding, determined in the presence of 1 μM LqhαIT, was subtracted. The K_i values (in nM, $n \geq 3$) are His-Av2, 0.41 ± 0.02; rAv2, 0.22 ± 0.14; nAv2, 0.4 ± 0.05; His-V2A, 4 ± 0.7; His-P3A, 1.1 ± 0.18; His-L5A, 11.2 ± 1.5; His-V13A, 0.85 ± 0.07; His-N16A, 4.6 ± 0.07; His-L18A, 85.5 ± 3.5; and His-I41A, 6.7 ± 0.1; the K_i ratios of the mutants are presented in Table 2. (B) Effects of representative mutations on the binding energy ($\Delta\Delta G$; see details in Table 2). The vertical line stands for a $\Delta\Delta G$ value of 1.3 kcal/mol, which is considered a minimum significant decrease in binding affinity. Residues whose substitution resulted in a higher value were considered important for binding and were assigned to the bioactive surface if their CD spectrum was similar to that of His-Av2 (see colored residues in Figure 6).

raise for the first time a role for *N*-terminal aliphatic residues in the bioactive surface of a sea anemone toxin. Although a D9A substitution had a detrimental effect on activity (Table 2), a D9N substitution had a smaller effect (5.8-fold) suggesting that the carboxyl of Asp-9 is not critical for activity.

Mutagenesis of the Arg-14 Loop and Its Vicinity. The Arg-14 loop is known for its flexibility (*5*, *31*), and whether this flexibility is related to toxin function is still an open question. Of the 10 residues that constitute this loop, substitutions N16A and most notably L18A strongly decreased the binding affinity (Table 2). These residues were shown to be important for ApB activity on mammalian Na_vs (*32*, *33*).

Mutagenesis of Gly residues in positions 10, 15, and 20 in ApB decreased the activity on the brain $Na_v1.2$ expressed in murine neuroblastoma and the human heart $Na_v1.5$ (*31*). These residues are conserved and seem to occupy key positions for the flexibility of the Arg-14 loop (*2*, *5*), and therefore, we substituted them to Ala and Pro. Although G20A severely affected the binding affinity and toxicity of Av2, the effect of G10A was limited, and G15A had an even a lower effect (Table 2). Whereas G15P did not affect the toxin activity, substitutions G10P and G20P severely damaged the binding affinity of Av2 (Table 2). However, because the CD spectrum of the latter two mutants was noticeably different from that of the unmodified toxin (Figure 4), this effect could result from structural perturbation. These results suggest that Gly-10 and Gly-20 may be important for maintaining the flexibility of the Arg-14 loop, as was previously suggested in ApB (*31*).

Role of Residues at the C-Terminal Half of Av2. No residues that are involved in bioactivity have been identified at the molecule central region. Expression of W23A and L24A mutants was unsuccessful, suggesting that these residues of the molecule core have a pivotal role in folding and toxin structure. This suggestion was corroborated by conservative substitutions W23F and L24V, which resulted in active recombinant toxins (not shown). At the *C*-terminal part of Av2, only substitution I41A noticeably affected (16-fold) the binding affinity and toxicity, indicating that Ile-41 might be involved in the bioactive surface of Av2 (Table 2).

Activity of Selected Av2 Mutants on the Human Heart Na-Channel. In light of the differences in residues that constitute

Table 2: Effects of Mutations in His-Av2 on the Binding Energy to Cockroach Neuronal Membranes[a]

toxin	K_i ratio	$\Delta\Delta G$ (kcal/mol)	toxin	K_i ratio	$\Delta\Delta G$ (kcal/mol)
His-Av2	1	0	His-S19A	3.7	0.74
rAv2	0.5	−0.36	His-G20A	21	1.73
His-V2A	9.8	1.32	His-G20P	43	*b*
His-P3A	2.7	0.57	His-I21A	3.2	0.66
His-L5A	27	1.88	His-P28A	0.7	−0.18
His-D7A	3	0.63	His-S29A	0.9	−0.08
His-S8A	4	0.79	His-W31A	3.7	0.74
His-D9A	317	3.28	His-H32A	1.1	0.08
His-G10A	8	1.18	His-N33A	2.3	0.47
His-G10P	160	*b*	His-K35A	1.8	0.33
His-S12A	1	0	His-K36A	1.2	0.1
His-V13A	2	0.4	His H37A	2.4	0.5
His-R14A	4	0.79	His-P39A	7.1	1.12
His-G15A	4.4	0.84	His-T40A	1.9	0.37
His-G15P	3.4	0.7	His-I41A	16	1.6
His-N16A	11	1.38	His-W43A	2.7	1
rT17A	1	0	His-Q47A	0.2	−0.79
His-L18A	209	3.04			

[a] The change in the apparent binding affinity of each mutant was obtained in competition with ^{125}I-LqhαIT scorpion toxin on binding to cockroach neuronal membranes and is presented as the K_i ratio (K_i^{mut} over K_i^{wt}; the K_i^{wt} is 0.41 ± 0.02; $n = 3$). The K_i determination is described in the Experimental Procedures and in Figure 3. Binding energy calculation is depicted in the Experimental Procedures. Values calculated for rAv2 mutants (L5A, S8A, G15A, N16A, L18A, S19A, I41A, and Q47A) are not included because they were essentially similar to those of their His-Av2 equivalents. [b] The $\Delta\Delta G$ of mutations that altered the CD spectrum was not calculated.

the anti-insect bioactive surface of Av2 (Table 2) compared to those reported to compose the anti-mammalian bioactive surface of ApB (*2*), we examined nine Av2 mutants on the human heart channel $Na_v1.5$ expressed in *Xenopus* oocytes (Experimental Procedures). It is noteworthy that $Na_v1.5$ was used for analysis of ApB because of its high sensitivity to sea anemone toxins (*14*, *16*). Using various concentrations of rAv2, we determined its EC_{50} value (209.4 ± 54.6 nM; $n = 4$; Figure 5A), and used slightly higher concentrations (300 nM) of the toxin mutants to assess their effect on channel inactivation. Whereas V2A, W31A, and K35A were almost as active as rAv2, substitutions L5A, L18A, and I41A strongly decreased the ability of the toxin to slow inactivation in $Na_v1.5$, and D9A, N16A, and S19A had moderate effects (Figure 5B). The results obtained have suggested that the anti-mammalian and anti-insect bioactive surfaces of Av2 are very similar and that they differ markedly from the bioactive surface of ApB.

DISCUSSION

Understanding the mechanism by which sea anemone toxins interact with the Na_v and how they compete with scorpion α-toxins on the same receptor site despite any structural resemblance requires the comparison of the toxin−receptor modes of interaction. Whereas the bioactive surface of scorpion α-toxins toward insects has been recently reported (*34*−*36*), the putative face of interaction of sea anemones with mammalian Na_vs is only partly known. Most of the data on the residues important for the activity of sea anemone toxins have been accumulated thus far by mutagenesis of the toxin ApB, with the objective of clarifying its preference for mammalian heart versus brain Na_v subtypes (*2*). The differences in preference for various mammalian

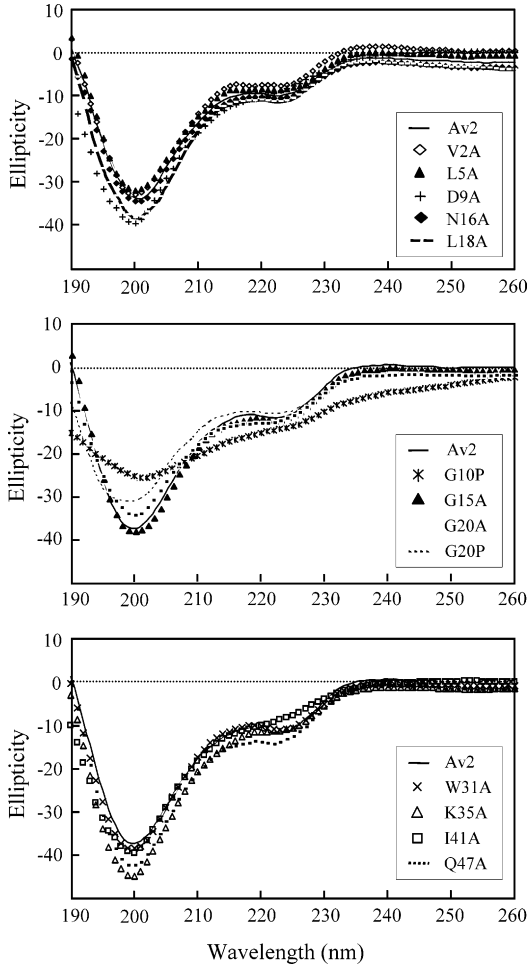

FIGURE 4: Circular dichroism spectra of His-Av2 variants. The spectra presented are of mutant representatives with altered activity: V2A, L5A, D9A, G10P, G20A, G20P, N16A, L18A, and Q47A. Nonaltered activity: G15A, W31A, and K35A. All toxin variants analyzed bear a His-tag.

Na_vs raise the question as to what extent the receptor site for sea anemone toxins is conserved and whether the bioactive surface of these toxins toward insects overlaps with that toward mammals.

As a first step toward the identification of the bioactive surface of sea anemone toxins toward insect Na_vs, we analyzed Av2, a highly potent insecticidal type I toxin (Table 1) by complete mutagenesis of its entire surface.

Av2 Presents a Similar Bioactive Surface toward Insects and Mammals. Six residues on the surface of Av2 have been identified as important for function in both toxicity to blowfly larvae and binding affinity for cockroach neuronal membranes (Val-2, Leu-5, Asp-9, Asn-16, Leu-18, and Ile-41; Table 2). Such strong correlation between the two distinct datasets may imply that they may be relevant for other insect families as well. Because the substitution of Leu-5, Leu-18, and Ile-41 severely decreased the toxin effect on the human $Na_v1.5$ channel, the substitution of Asp-9 and Asn-16 had moderate effects, and mutant V2A had only a minor effect (Figure 5B), we conclude that the anti-insect and anti-mammalian bioactive surfaces of Av2 are very similar. The importance of Asp-9, Asn-16, and Leu-18 equivalents in ApB toward mammalian Na_vs has been reported (*32*, *33*, *37*), and the bioactive role of Asn-16 in Type I sea anemone toxins toward both mammals and insects was also implicated from

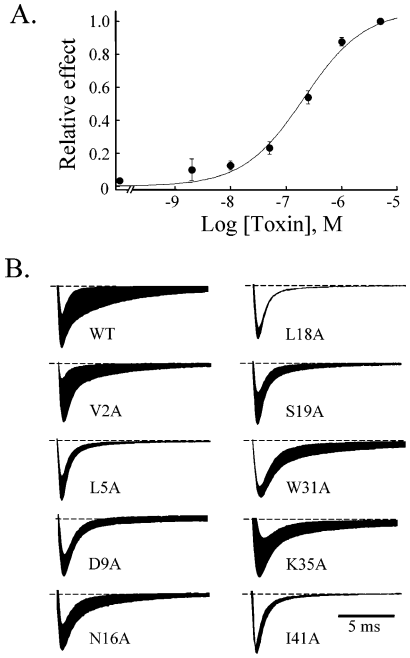

FIGURE 5: Effects of rAv2 and its mutants on the human channel $Na_v1.5$. (A) Dose−response curve of rAv2 effect on fast inactivation of $Na_v1.5$. Oocytes expressing $Na_v1.5$ were clamped at −80 mV, and currents were elicited by step depolarization to −10 mV. Increasing concentrations of rAv2 (up to 5 μM) were applied and their relative effect on the currents at −10 mV yielded an EC_{50} of 209.4 ± 54.6 nM ($n = 4$). (B) Alterations in the current induced by rAv2 mutants upon a depolarizing test pulse to −10 mV from a −80 mV holding potential. The concentration of rAv2 was 250 nM and that of the mutants, 300 nM. The shaded areas illustrate the increase in current upon toxin application.

a less active natural variant of this position in Bg III (Asp-16) compared to Bg II (Asn-16) (Figure 1; *19*, *38*).

The importance of Leu-5 and Ile-41 for the activity of a sea anemone toxin toward insects and mammals is reported for the first time. The role of Ile-41 in ApB activity could not be assessed because of difficulties in the folding of its nonconservative mutants (*33*). Av2 I41A, however, folded well (Figure 4). The substantial conservation of these residues suggests that they may play a role in the bioactive surfaces of other sea anemone toxins (Figure 1).

Analysis of ApB on mammalian $Na_v1.2$ and $Na_v1.5$ channels has revealed that in addition to Asn-16 and Leu-18, Arg-12, Ser-19, Trp-33, Lys-37, and Lys-49 are important for activity on both channel types (*2*). Av2 and ApB are 79% identical, and all residues important for activity excluding Arg-12 and Lys-49 appear in both (Figure 1). However, Ser-19 seems to be important for the anti-mammalian activity (Figure 5B) but has a negligible effect on the activity of Av2 toward insects (Table 2). A major variation between the bioactive surfaces of ApB and Av2 is exhibited by Trp-33 and Lys-37 in ApB compared to their Trp-31 and Lys-35 equivalents in Av2 (Figure 1). Although Lys-37 in ApB was suggested to interact directly with Asp-1612 of $Na_v1.5$ (*18*), and even a conservative substitution of Trp-33 demolished ApB activity (*39*), substitution of their Av2 equivalents had no effect on the insecticidal activity (Table 2) and only slightly affected the activity on $Na_v1.5$ (Figure 5B). Of the four aliphatic residues with bioactive roles on the surface of Av2 (Figure 6), only Leu-18 was ascribed to the anti-mammalian bioactive surface of ApB. These glaring differences in the bioactive surfaces imply that despite some commonality at the Arg-14 loop, the surface of interaction of Av2 with receptor site-3 differs from that of ApB with site-3 on mammalian Na_vs. This assumption is corroborated by the proposal of Benzinger et al. (*40*) stating that the binding sites of ApA and ApB on rat skeletal muscle and cardiac Na_vs differ to some extent.

Putative Characteristics of the Receptor Site for Av2. Rogers et al. have proposed that D4/S3−S4 is part of receptor site-3 on $Na_v1.2a$ (*9*). A few conserved aliphatic residues on this loop such as Val-1620 and Leu-1624 were proposed to affect the interaction of Av2 with the channel. Because four of the six bioactive residues on the surface of Av2 are aliphatic, they may be suitable candidates for the interaction with the aliphatic D4/S3−S4 residues. The apparent commonality in residues that constitute both the anti-insect and anti-mammalian bioactive surfaces of Av2 may suggest that their receptor sites on insect and mammalian Na_vs are conserved. Moreover, most substitutions in D4/S3−S4 that significantly affected the binding of Av2 had no effect on the binding of the scorpion α-toxin Lqq5 (*9*). By extrapolation, these mismatches are seemingly in accordance with the noticeable differences between the bioactive surface of Av2 described in this work and the bioactive surfaces toward insects of LqhαIT and other scorpion α-toxins (*34*−*36*). The bioactive surface of Av2 is devoid of cationic and aromatic residues, which appear on the bioactive surface of scorpion α-toxins. In addition, the bioactive surface of scorpion α-toxins consists of well-organized amino acid clusters (*35*, *36*, *41*), whereas the bioactive residues on the surface of Av2 are dispersed. This major difference is reflected by the lack of satisfactory results in structural model alignments of Av2 and scorpion α-toxins based on their functional residues (data not shown). The differences both in the bioactive surfaces and the residues in the Na_v, which affect toxin binding to the channel, may imply that the binding sites of sea anemone toxins and scorpion α-toxins only partly overlap. Such a suggestion is in concert with our perspective about receptor site-3, which may be considered a macrosite whose boundaries are defined by a collection of channel modifiers that compete on binding and render a similar physiological effect (*8*). A comparison of two different bioactive surfaces that compete with one another on the same binding site, followed in the long range by elucidation of channel residues that participate in these interactions, may provide structural details about macrosite-3.

Putative Role of the Arg-14 Loop. The flexibility of the Arg-14 loop is evident from the wide root-mean-square deviation detected in the NMR structures of a number of type I and type II sea anemone toxins (*42*−*45*). The conservation of Gly-10 and Gly-20 on both sides of the loop (Figure 1) accentuates the putative significance for free movement. Indeed, the mutagenesis of these Gly residues, especially Gly-20, decreased toxin activity (*31*) (Table 2). The importance of these glycines as well as Gly-15 at the loop center for ApB activity was previously noted (*31*). Our results indicate that Gly-15 is not essential for the activity or binding of Av2 in insects. Another difference between both toxins is that whereas substitution of Gly-20 by Ala affected the CD spectrum of ApB (*31*), it did not affect the CD spectrum of Av2. Such a difference is surprising in light of the similarity and conservation of the Arg-14 loop in both

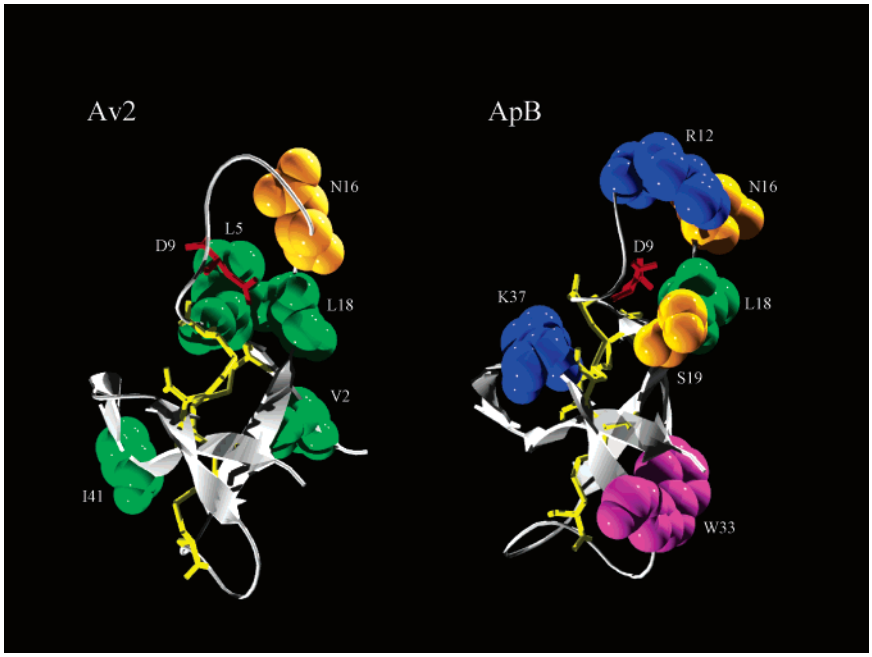

FIGURE 6: Bioactive surface of Av2 compared to that of ApB. A view of the residues that form the functional surfaces of Av2 and ApB. Amino acid residues assigned to the bioactive surface are shown in space fill format and are colored according to their chemical nature. The amino acids carrying aromatic side chains are colored magenta; those with aliphatic side chains in green; those with polar side chains in orange; positively charged residues in blue; and negatively charged in red. Because the bioactive role of Asp-9 is unclear, it is presented in sticks format. The structure of ApB is from Protein Data Bank accession 1 APF, and that of Av2 is a model based on the structure of three Type 1 and a Type II sea anemone toxins (see Experimental Procedures).

toxins. Interestingly, the substitution of Gly-10 or Gly-20 by Pro changed the CD spectrum of Av2, whereas substitutions to Ala did not (Figure 4). It is likely that the introduction of Pro to these positions increases the rigidity of the Arg-14 loop. Hence, the freedom of tilting is seemingly an important feature of the Arg-14 loop and together with the bioactive role of residues 16 and 18 suggests that this flexibility is somehow essential for the interaction with the receptor site.

Another residue whose substitution by Ala affects toxin action is the conserved Asp-9 (Table 2; Figure 1**)**, as was also reported with Asp-9 of ApB (*37*). Because substitution D9N had only a small effect on toxicity, the carboxyl group of Asp-9 is not critical for Av2 activity. As may be inferred from the NMR structures of ApA and ApB, a hydrogen bond exists between the carbonyl group at the side chain of Asp-9 and the amine of Cys-6 (*42*, *43*). Theoretically this bond should be maintained when the Asp is substituted by Asn. Khera and Blumenthal (*37*) reported that Asp-9 is critical for the proper folding of ApB on the basis of the prominent decline in polypeptide yield when mutated at this position. However, we did not encounter the same phenomenon in Asp-9 mutants of Av2. Because the CD spectra of mutants at Asp-9 and the unmodified toxin were similar (Figure 4), we presume that mutations in Asp-9 did not affect the structure of Av2, at least in a way noticeable by the analysis of CD spectra. Therefore, we suggest that the role of the hydrogen bond formed by the carbonyl of Asp-9 with Cys-6 is to limit the free tilting of the Arg-14 loop. If we further assume that the binding of sea anemone toxins to receptor site-3 includes a step of induced fit (*46*, *47*), which involves the Arg-14 loop, it is possible that its flexibility enables the adoption of a shape necessary for binding. An indirect support of this assumption may be drawn from the very slow association rate of sea anemone toxins to their receptor (*40*), the delayed symptoms observed in injected blowfly larvae, and the long duration before the maximal effect of Av2 on $DmNa_v1$ and $Na_v1.5$ is reached (not shown). Yet, it cannot be ruled out that the carbonyl of Asp-9 simply interacts with the Na_v receptor site.

In summary, this work provides for the first time a full survey of the bioactive surface of the sea anemone toxin Av2 toward insect Na_vs. Although this surface seems to affect mammalian Na_vs as well, it differs markedly from the anti-mammalian bioactive surface described previously for ApB (*2*) and the bioactive surface of scorpion α-toxins (*35*, *41*). This work corroborates once more the putative bioactive role of the Arg-14 loop, whose mode of interaction with the channel receptor remains to be described.

ACKNOWLEDGMENT

We thank Dr. R. Thai from DIEP, CEA Saclay, France, for his help in amino acid analysis. Vectors encoding the human $Na_v1.5$, $DmNa_v1$ sodium channel α-subunit, and the auxiliary TipE subunit were kindly provided by Prof. R. G. Kallen, University of Pennsylvania, PA and Dr. J. W. Warmke, Merck, NJ, and Dr. M. S. Williamson, IACR-Rothamsted, U.K., respectively.

REFERENCES

1. Whittington, H. B. (1985) *The Burgess Shale*, Yale University Press, New Haven, CT.
2. Blumenthal, K. M., and Seibert, A. L. (2003) Voltage-gated sodium channel toxins: poison, probes, and future promise, *Cell. Biochem. Biophys. 38*, 215−238.
3. Catterall, W. A. (1992) Cellular and molecular biology of voltage-gated sodium channels, *Physiol. Rev. 72*, 15−48.
4. Catteral, W. A., Goldin, A. L., and Waxman, S. G., (2003) International union of pharmacology, XXXIX, compendium of

voltage-gated ion channels: sodium channels, *Pharmacol. Rev. 55*, 575−578.
5. Norton, R. S. (1991) Structure−function relationships of sea anemone proteins that interact with the sodium channel, *Toxicon 29*, 1051−1084.
6. Catterall, W. A., and Beress, L. (1978) Sea anemone toxin and scorpion toxin share a common receptor site associated with the action potential sodium ionophore, *J. Biol. Chem. 253*, 7393−7396.
7. Gordon, D., and Zlotkin, E. (1993) Binding of alpha scorpion toxin to insect sodium channels is not dependent on membrane potential, *FEBS Lett. 315*, 125−128.
8. Gordon, D., Martin-Eauclaire, M.-F., Cestele, S., Kopeyan, C., Carlier, E., Ben Khalifa, R., Pelhate, M., and Rochat, H. (1996) Scorpion toxins affecting sodium current inactivation bind to distinct homologous receptor sites on rat brain and insect sodium channels, *J. Biol. Chem. 271*, 8034−8045.
9. Rogers, J. C., Qu, Y., Tanada, T. N., Scheuer, T., and Catterall, W. A. (1996) Molecular determinants of high affinity binding of α-scorpion toxin and sea anemone toxin in the S3−S4 extracellular loop in domain IV of the Na^+ channel α subunit, *J. Biol. Chem. 271*, 15950−15962.
10. Beress, L., Beress, R., and Wunderer G. (1975) Isolation and characterization of three polypeptides with neurotoxic activity from *Anemonia sulcata*, *FEBS Lett. 50*, 311−314.
11. Csaba, G., Dobozy, O., Darvas, Z., Laszlo, V., and Beress, L. (1984) Phylogenetic change in sensitivity to *Anemonia sulcata* toxin (ATX II), and impact of first interaction with the toxin (imprinting) on later response to it, *Comp. Biochem. Physiol., C. 77*, 153−155.
12. Warmke, J. W., Reenan, A. G. R., Wang, P., Qian, S., Arena, J. P., Wang, J., Wunderler, D., Liu, K., Kaczorowski, G. J., Van der Ploeg, L. H. T., Ganetzky, B., and Cohen, C. J. (1997) Functional expression of *Drosophila para* sodium channels. Modulation by membrane protein TipE and toxin pharmacology, *J. Gen. Physiol. 110*, 119−133.
13. Alsen, C., Beress, L., Fischer, K., Proppe D., Reinberg, T., and Sattler, R. W. (1976) The action of a toxin from the sea anemone *Anemonia sulcata* upon mammalian heart muscles, *Naunyn-Schmiedeberg's Arch. Pharmacol. 295*, 55−62.
14. Chahine, M. Plante, E., and Kallen, R. G. (1996) Sea anemone toxin (ATX II) modulation of heart and skeletal muscle sodium channel alpha-subunits expressed in tsA201 cells, *J. Membr. Biol. 152*, 39−48.
15. Barhanin, J., Hugues, M., Schweitz, H., Vincent, J.-P., and Lazdunski, M. (1981) Structure−function relationships of sea anemone toxin II from *Anemonia sulcata*, *J. Biol. Chem. 256*, 5764−5769.
16. Gallagher, M. J., and Blumenthal, K. M. (1992) Cloning and expression of wild-type and mutant forms of the cardiotonic polypeptide Anthopleurin B, *J. Biol. Chem. 267*, 13958−13963.
17. Wang, L., Ou, J., Peng, L., Zhong, X., Du, J., Liu, Y., Zhang, Y., Dong, M., and Xu, A.-L. (2004) Functional expression and characterization of four novel neurotoxins from sea anemone *Anthopleura* sp, *Biochem. Biophys. Res. Commun. 313*, 163−170.
18. Benzinger, G. R., Kyle, J. W., Blumenthal, K. M., and Hanck, D. A. (1998) A specific interaction between the cardiac sodium channel and site-3 toxin Anthopleurin B, *J. Biol. Chem. 273*, 80−84.
19. Loret, E. P., Menendez, R., Mansuelle, P., Sampieri, F., and Rochat, H. (1994) Positively charged amino acid residues located similarly in sea anemone and scorpion toxins, *J. Biol. Chem. 269*, 16785−16788.
20. Froy, O., Zilberberg, N., Gordon, D., Turkov, M., Gilles, N., Stankiewicz, M., Plehate, M., Loret, E., Oren, D. A., Shaanan, B., and Gurevitz, M. (1999) The putative bioactive surface of insect-selective scorpion excitatory neurotoxins, *J. Biol. Chem. 274*, 5769−5776.
21. Cohen, L., Karbat, I., Gilles, N., Ilan, N., Benveniste, M., Gordon, D., and Gurevitz, M. (2005) Common features in the functional surface of scorpion β-toxins and elements that confer specificity for insect and mammalian voltage-gated sodium channels, *J. Biol. Chem. 280*, 5045−5053.
22. Wunderer, G., Fritz, H., Wachter, E., and Machleidt, W. (1976) Amino acid sequence of a coelenterate toxin: toxin II from *Anemonia sulcata*, *Eur. J. Biochem. 68*, 193−198.
23. Turkov, M., Rashi, S., Zilberberg, N., Gordon, D., Ben-Khalifa, R., Stankiewicz, M., Pelhate, M., and Gurevitz, M. (1997) In vitro folding and functional analysis of an anti-insect selective scorpion depressant neurotoxin produced in *Escherichia coli*, *Protein Expression Purif. 10*, 123−131.
24. Reed, L., and Muench, H. (1938) A simple method of estimating fifty-percent endpoint, *Am. J. Hyg. 27*, 493−497.
25. Gilles, N., Krimm, I., Bouet, F., Froy, O., Gurevitz, M., Lancelin, J.-M., and Gordon, D. (2000) Structural implications on the interaction of scorpion α-like toxins with the sodium channel receptor site inferred from toxin iodination and pH-dependent binding, *J. Neurochem. 75*, 1735−1745.
26. Rochat, C., Tessier, M., Miranda, F., and Lissitzky, S. (1977) Radioiodination of scorpion and snake neurotoxins, *Anal. Biochem. 82*, 532−548.
27. Gershon, E., Weigl, L., Lotan, I., Schreibmayer, W., and Dascal, N. (1992) Protein kinase A reduces voltage-dependent Na^+ current in *Xenopus* oocytes, *J. Neurosci. 12*, 3743−3752.
28. Wallner, M., Weigl, L., Meera, P., and Lotan, I. (1993) Modulation of the skeletal muscle sodium channel alpha-subunit by the beta-1 subunit, *FEBS Lett. 336*, 535−539.
29. Shichor, I., Zlotkin, E., Ilan, N., Chikashvili, D., Stuhmer, W., Gordon, D., and Lotan, I. (2002) Domain 2 of Drosophila para voltage-gated sodium channel confers insect properties to a rat brain channel, *J. Neurosci. 22*, 4364−4371.
30. Schwede, T., Kopp, J., Guex, N., and Peitsch, M. C. (2003) SWISS-MODEL: an automated protein homology-modeling server, *Nucleic Acids Res. 31*, 3381−3385.
31. Seibert, A. L., Liu, J., Hanck, D. A., and Blumenthal, K. M. (2003) Arg-14 loop of site 3 anemone toxins: effects of glycine replacement on toxin affinity, *Biochemistry 42*, 14515−14521.
32. Seibert, A. L. Liu, J., Hanck, D. A., and Blumenthal, K. M. (2004) Role of Asn-16 and Ser-19 in Anthopleurin B binding. Implication for the electrostatic nature of Na_v site 3, *Biochemistry 43*, 7082−7089.
33. Dias-Kadambi, B. L., Drum, C. I., Hanck, D. A., and Blumenthal K. M. (1996) Leucine 18, a hydrophobic residue essential for high affinity binding of Anthopleurin B to the voltage-sensitive sodium channel, *J. Biol. Chem. 271*, 9422−9428.
34. Wang, C. G., Gilles, N., Hamon, A., Le Gall, F., Stankiewicz, M., Pelhate, M., Xiong, Y. M., Wang, D. C., and Chi C. W. (2003) Exploration of the functional site of a scorpion alpha-like toxin by site-directed mutagenesis, *Biochemistry*, *42*, 4699−4708.
35. Karbat, I., Frolow, F., Froy, O., Gilles, N., Cohen, L., Turkov, M., Gordon, D., and Gurevitz, M. (2004) Molecular basis of the high insecticidal potency of scorpion alpha-toxins, *J. Biol. Chem. 279*, 31679−31686.
36. Liu, L., Bosmans, F., Maertens, C., Zhu, R. H., Wang, D. C., and Tytgat, J. (2005) Molecular basis of the mammalian potency of the scorpion alpha-like toxin, BmK M1, *FASEB J. 19*, 594−596.
37. Khera, P. K., and Blumenthal, K. M. (1996) Importance of highly conserved anionic residues and electrostatic interactions in the activity and structure of the cardiotonic polypeptide Anthopleurin B, *Biochemistry 35*, 3503−3507.
38. Bosmans, F., Aneiros, A., and Tytgat, J. (2002) The sea anemone *Bunodosoma granulifera* contains surprisingly efficacious and potent insect-selective toxins, *FEBS Lett. 532*, 131−134.
39. Dias-Kadambi, B. L., Combs, K. A., Drum, C. L., Hanck, D. A., and Blumenthal, K. M. (1996) The role of exposed tryptophan residues in the activity of the cardiotonic polypeptide Anthopleurin B, *J. Biol.* Chem. *271*, 23828−23835.
40. Benzinger, G. R., Drum, C. L., Chen, L.-Q., Kallen, R. G., and Hanck, D. A. (1997) Differences in the binding sites of two site-3 sodium channel toxins, *Pflugers Arch. 424*, 742−749.
41. Ali, S. A., Wang, B., Alam, M., Beck, A., Stoeva, S., Voelter, W., Abbasi, A., and Duszenko, M. (2006) Structure−activity relationship of an alpha-toxin Bs-Tx28 from scorpion (*Buthus sindicus*) venom suggests a new alpha-toxin subfamily, *Arch. Biochem. Biophys. 445*, 81−94.
42. Pallaghy, P. K., Scanlon, M. J., and Norton, R. S. (1995) Three-dimensional structure in solution of the polypeptide cardiac stimulant Anthopleurin-A, *Biochemistry 34*, 3782−3794.
43. Monks, S. A., Pallaghy, P. K., Scanlon, M. J., and Norton, R. S. (1995) Solution structure of the cardiostimulant polypeptide Anthopleurin-B and comparison with Anthopleurin-A, *Structure 15*, 791−803.
44. Fogh, R. H., Kem, W. R., and Norton R. S. (1990) Solution structure of neurotoxin I from the sea anemone *Stichodactyla helianthus*. A nuclear magnetic resonance, distance geometry, and restrained molecular dynamics study, *J. Biol. Chem. 265*, 13016−13028.

45. Wilcox, G. R., Fogh, R. H., and Norton, R. S. (1993) Refinement of the solution structure of the sea anemone neurotoxin Sh I, *J. Biol. Chem. 268*, 24707−24719.
46. Koshland, D. E. (1958) Application of a theory of enzyme specificity to protein synthesis, *Proc. Natl. Acad. Sci. U.S.A. 44*, 98−104.
47. Buck, E., and Iyengar, R. (2003) Organization and functions of interacting domains for signaling by protein−protein interactions. *Sci. STKE 209*, 14−18.

BI060386B